Interfacing Synchronous Machine Model Including Stator Transients with Network for Stability Studies

Bandopant Pawar, *Student Member, IEEE,* Efstratios I. Batzelis, *Senior Member, IEEE,*
Saikat Chakrabarti, *Senior Member, IEEE,* and Bikash C. Pal, *Fellow, IEEE*

***Abstract*—A detailed multi-time scale model of synchronous machines (SM) with stator transients is necessary to capture the complex interactions in inverter-integrated power systems. The conventional detailed SM model, including stator transients, is incompatible with that of the step-up transformer in the dq domain as both are modeled as current sources in series. This letter proposes an efficient approach for interfacing the detailed SM model with the transformer by reformulating the SM model as a voltage source without accuracy loss. MATLAB/Simulink numerical simulations using New England 39-bus test system validate the computational efficiency of the proposed approach.**

***Index Terms*—Accuracy, *dq* model, network dynamics, power system stability, simulation, stiffness, synchronous machine.**

I. Introduction

THE conventional *phasor* tools fail to capture the complex inverter interactions with the grid [1], whereas, more accurate *electromagnetic transient (EMT)* programs are complex and less user-friendly for large-size networks. Hence, the *dq* domain approach with detailed network dynamics and balanced operating points is becoming popular for stability analysis of inverter-integrated power systems [1], [2]. Furthermore, neglecting synchronous machine (SM) stator transients, as in the case of *phasor* approach, may fail to capture the faster interactions with inverter controls [1]. Hence, a detailed SM modeling with stator transients is necessary for reliable stability studies of inverter-integrated power systems [1].

The widely used eighth-order SM model with stator transients in *dq* domain [3] represents the SM as a voltage-dependent current source. The current source representation of SM results in incompatible formulation with a step-up transformer, also modeled as a current source, in series, due to the implicit terminal voltage variable [4].

There are some *indirect* interfacing methods for the *dq* approach, such as the inclusion of a snubber resistance and time step relaxation [4]. The time step relaxation decouples the network dynamics from the SM model with data exchange only once every time step [4]. However, this approach is numerically stable for small time steps, it is suitable for time-domain simulations only, rather than overall stability studies, including small-signal analysis. In contrast, the snubber resistance approach is widely applicable, but at the cost of additional computational complexity [4], as shown later. Interfacing the detailed SM model to a dynamic network model in *dq* domain remains an unresolved issue. Existing methods compromise either in accuracy or computational complexity.

TABLE I
Comparison of the proposed approach with VBR models

Reference	Stator interface	Rotor interface	Circuit parameter	Algebr. loop	Parameters used
[6]	Direct	Indirect	Variable	No	Actual
[7]	Direct	Indirect	Constant	No	Actual
[8]	Direct	Direct	Variable	No	Actual
[9]	Direct	Direct	Constant	Yes	Actual
Proposed	Direct	Direct	Constant	No	Operational

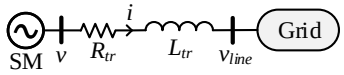

Fig. 1. A schematic of a grid connected synchronous machine.

Such incompatibility issues in EMT programs have been addressed with *direct* interfacing approaches, such as *phase domain* and *voltage behind reactance* (VBR) models [4], [5]. However, these direct approaches are well suited for the detailed EMT time-domain simulations in *abc* coordinates [5]. Table I shows that the VBR approaches in the literature [6]–[9], focusing on EMT simulations, have at least one limitation, e.g., indirect stator or rotor interface, time-varying circuit parameters, and algebraic loops. Furthermore, the existing VBR approaches [6]–[9] use actual circuit parameters. We are still missing a computationally efficient compatible formulation for SM and transformer models in the *dq*-domain in terms of SM operational parameters, suitable for stability studies.

This letter presents a direct approach to interface the detailed SM model with the network, considering stator transients. The proposed method reformulates the multi-time scale SM model as a voltage source behind the sub-transient reactance with no accuracy loss and reduced computational complexity. The proposed formulation results in direct interfacing for the stator and rotor circuits and has constant circuit parameters; it does not involve algebraic loops; it is compatible with the existing phasor tools due to operational parameters [3], especially for using the structure-preserving reduced-order models, if required. The proposed approach is most suited for dynamics studies of inverter-based power systems.

MATLAB/Simulink case studies with New England 39-bus test system validate the effectiveness of the proposed approach.

II. Multi-Time Scale Synchronous Machine Model

Fig. 1 shows a schematic of an SM connected via a step-up transformer, where R_{tr} and L_{tr} are the transformer equivalent resistance and series inductance; v, v_{line} are the SM terminal and adjacent line voltage, respectively. A detailed eighth-order multi-time scale model of a grid-connected SM, shown in Fig.

This work was supported by the Royal Academy of Engineering through the Engineering for Development Research Fellowship scheme under the Grant RF\201819\18\86.

(Corresponding author: Bandopant Pawar)

B. Pawar and S. Chakrabarti are with the Department of Electrical Engineering, Indian Institute of Technology Kanpur, Uttar Pradesh 208016, India (e-mails: pawarbb@iitk.ac.in; saikatc@iitk.ac.in).

Efstratios I. Batzelis is with the School of Electronics and Computer Science, University of Southampton, Southampton, SO17 1BJ, UK (e-mail: e.batzelis@soton.ac.uk). Bikash C. Pal is with the Department of Electrical and Electronic Engineering, Imperial College, London SW7 2AZ, U.K. (e-mail: b.pal@imperial.ac.uk).

1, with stator transients in terms of standard parameters is given by (1)-(10) [3], [10].

$$-\tfrac{1}{\omega_b}\tfrac{d\psi_d}{dt} = R_a i_d + \tfrac{\omega}{\omega_b}\psi_q + v_d \quad (1)$$

$$-\tfrac{1}{\omega_b}\tfrac{d\psi_q}{dt} = R_a i_q - \tfrac{\omega}{\omega_b}\psi_d + v_q \quad (2)$$

$$T'_{q0}\tfrac{de'_d}{dt} = -e'_d + (X_q - X'_q)\{-i_q + \tfrac{(X'_q - X''_q)}{(X'_q - X_{ls})^2}((X'_q - X_{ls})i_q - e'_d - \psi_{2q})\} \quad (3)$$

$$T'_{d0}\tfrac{de'_q}{dt} = e_{fd} - e'_q + (X_d - X'_d)\{i_d + \tfrac{(X'_d - X''_d)}{(X'_d - X_{ls})^2}((X_{ls} - X'_d)i_d - e'_q + \psi_{1d})\} \quad (4)$$

$$T''_{q0}\tfrac{d\psi_{2q}}{dt} = -e'_d + (X'_q - X_{ls})i_q - \psi_{2q} \quad (5)$$

$$T''_{d0}\tfrac{d\psi_{1d}}{dt} = e'_q + (X'_d - X_{ls})i_d - \psi_{1d} \quad (6)$$

$$\tfrac{d\delta}{dt} = \omega - \omega_c \quad (7)$$

$$\tfrac{2H}{\omega_b}\tfrac{d\omega}{dt} = T_m - (\psi_d i_q - \psi_q i_d) - D'\tfrac{\omega}{\omega_b} \quad (8)$$

$$\psi_d = X''_d i_d + \tfrac{(X''_d - X_{ls})}{(X'_d - X_{ls})}e'_q + \tfrac{(X'_d - X''_d)}{(X'_d - X_{ls})}\psi_{1d} \quad (9)$$

$$\psi_q = X''_q i_q - \tfrac{(X''_q - X_{ls})}{(X'_q - X_{ls})}e'_d + \tfrac{(X'_q - X''_q)}{(X'_q - X_{ls})}\psi_{2q} \quad (10)$$

A dynamic model of the transformer is given by [2], [3],

$$L_{tr}\tfrac{di_q}{dt} = v_q - v_{qline} - R_{tr}i_q + \omega L_{tr} i_d \quad (11)$$

$$L_{tr}\tfrac{di_d}{dt} = v_d - v_{dline} - R_{tr}i_d - \omega L_{tr} i_q \quad (12)$$

The notations (in p.u. instantaneous values, unless specified) are as follows: ω_b, ω, ω_c are the base, rotor, and common reference frame speeds in rad/s; ψ_d, ψ_q are equivalent flux linkages; i_d, i_q are stator currents; v_d, v_q are stator terminal voltages; e'_q, e'_d are transient emfs; e_{fd} is the field excitation voltage; ψ_{1d}, ψ_{2q} are sub-transient damper flux linkages; T_m is the input mechanical torque.

III. Interfacing of SM Model with the Network

The SM model (1)-(10) is a voltage-controlled current source representation [3], [4], as it is in the form of flux linkages as states, and the terminal voltages as the input. The injected currents (9)-(10) are the algebraic variables in terms of flux linkages and internal voltages. The transformer model (11)-(12) is also a controlled current source that requires machine terminal and line voltage as inputs. The cascade connection of two current source models is an incompatible differential algebraic equation (DAE) formulation [4], as shown in Fig. 2(a), as none of the models give the machine terminal voltage as the output. A compatible DAE formulation for the SM and transformer model can be achieved using either direct or indirect interfacing approaches.

A. Indirect Approach using Snubber

The snubber resistor approach illustrated Fig. 2(b) is a widely used indirect method [4]. A resistor with large resistance, R_{snub}, connected across the SM terminals enables the computation of SM terminal voltage. The accuracy of this method increases with R_{snub} value, but this results in higher model stiffness and increased computational complexity [4].

B. Proposed Direct Approach

In the proposed direct approach, the machine model is reformulated in such a way that it is compatible with the external network, but without any accuracy loss. Rearranging the SM equations (1)-(2),

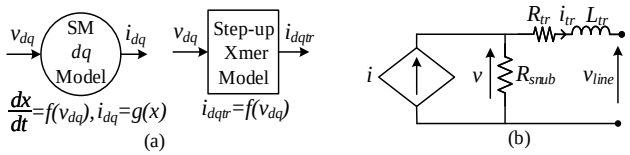

Fig. 2. (a) Incompatible interconnection of SM and step-up transformer models, (b) a schematic of SM representation with a snubber resistor.

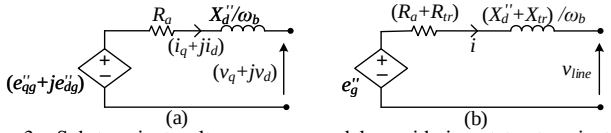

Fig. 3. Sub-transient voltage source model considering stator transients for (a) SM, (b) combined SM and step-up transformer.

$$-\tfrac{1}{\omega_b}\tfrac{d\psi_d}{dt} - \tfrac{\omega}{\omega_b}\psi_q = R_a i_d + v_d \quad (13)$$

$$-\tfrac{1}{\omega_b}\tfrac{d\psi_q}{dt} + \tfrac{\omega}{\omega_b}\psi_d = R_a i_q + v_q \quad (14)$$

The left hand side of (13)-(14) is the sub-transient generated voltage along the d and q axis. Rewriting (9)-(10),

$$\psi_d = X''_d i_d + \psi'_d, \psi_q = X''_q i_q + \psi'_q \quad (15)$$

$$\psi'_d = \tfrac{(X''_d - X_{ls})}{(X'_d - X_{ls})}e'_q + \tfrac{(X'_d - X''_d)}{(X'_d - X_{ls})}\psi_{1d} \quad (16)$$

$$\psi'_q = -\tfrac{(X''_q - X_{ls})}{(X'_q - X_{ls})}e'_d + \tfrac{(X'_q - X''_q)}{(X'_q - X_{ls})}\psi_{2q} \quad (17)$$

From (13)-(14) and (15)-(17),

$$-\tfrac{1}{\omega_b}\tfrac{d\psi'_d}{dt} - \tfrac{\omega}{\omega_b}\psi'_q = R_a i_d + v_d + \tfrac{X''_d}{\omega_b}\tfrac{di_d}{dt} + \tfrac{\omega}{\omega_b}X''_q i_q \quad (18)$$

$$-\tfrac{1}{\omega_b}\tfrac{d\psi'_q}{dt} + \tfrac{\omega}{\omega_b}\psi'_d = R_a i_q + v_q + \tfrac{X''_q}{\omega_b}\tfrac{di_q}{dt} - \tfrac{\omega}{\omega_b}X''_d i_d \quad (19)$$

For round rotor SMs, $X''_q = X''_d$. Hence, (18)-(19) represent a *voltage source* model for the SM behind an impedance, as shown in Fig. 3(a) and rewritten to (20)-(21),

$$e''_{dg} = R_a i_d + v_d + \tfrac{X''_d}{\omega_b}\tfrac{di_d}{dt} + \tfrac{\omega}{\omega_b}X''_d i_q \quad (20)$$

$$e''_{qg} = R_a i_q + v_q + \tfrac{X''_d}{\omega_b}\tfrac{di_q}{dt} - \tfrac{\omega}{\omega_b}X''_d i_d \quad (21)$$

$$\text{where, } e''_{dg} = -\tfrac{1}{\omega_b}\tfrac{d\psi'_d}{dt} - \tfrac{\omega}{\omega_b}\psi'_q, e''_{qg} = -\tfrac{1}{\omega_b}\tfrac{d\psi'_q}{dt} + \tfrac{\omega}{\omega_b}\psi'_d \quad (22)$$

Here, e''_{dg}, e''_{qg} are the generated sub-transient voltages. The voltage source model of round rotor SM shown in Fig. 3(a) still requires the machine terminal voltage as input. If we combine the SM model shown in Fig. 3(a) with the transformer model given by (11)-(12), we get rid of the machine terminal voltage, resulting in Fig. 3(b). The final voltage equations for the combined round rotor SM and transformer are given by,

$$e''_{dg} = (R_a + R_{tr})i_d + \tfrac{(X''_d + X_{tr})}{\omega_b}\tfrac{di_d}{dt} + \tfrac{\omega}{\omega_b}(X''_d + X_{tr})i_q + v_{dline} \quad (23)$$

$$e''_{qg} = (R_a + R_{tr})i_q + \tfrac{(X''_d + X_{tr})}{\omega_b}\tfrac{di_q}{dt} - \tfrac{\omega}{\omega_b}(X''_d + X_{tr})i_d + v_{qline} \quad (24)$$

However, the assumption of $X''_q = X''_d$ is not valid in case of the salient pole SM and saliency is to be considered for accurate representation of machine dynamics. The sub-transient stator saliency on account of unequal sub-transient reactances can be handled using a dummy rotor coil [10] on the q axis. Dynamics of the dummy coil and the d-axis transient emf considering the rotor saliency are given by [10],

$$T_c\tfrac{de'_{dc}}{dt} = -e'_{dc} + (X''_d - X''_q)i_q \quad (25)$$

$$e''_{dg} = -\tfrac{1}{\omega_b}\tfrac{d\psi'_d}{dt} - \tfrac{\omega}{\omega_b}\psi'_q + e'_{dc} \quad (26)$$

Here, e'_{dc} is the fictitious voltage generated due to the dummy

TABLE II
SUMMARY OF COMBINED MODELS OF SM AND STEP-UP TRANSFORMERS

SM Type	Indirect Approach		Direct Approach	
	Order	Eq. no.	Order	Eq. no.
Round rotor	10	(1)-(8), (11)-(12)	8	(3)-(8), (23)-(24)
Salient Pole	10	(1)-(8), (11)-(12)	9	(3)-(8), (23)-(25)

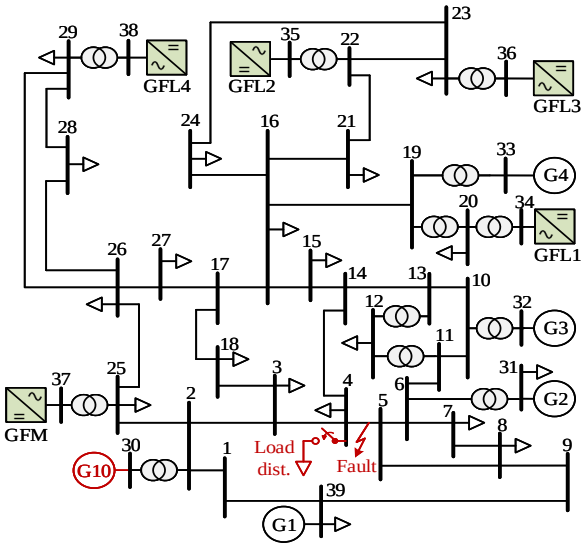

Fig. 4. New England 39-bus test system with SM-GFM-GFL generator combination.

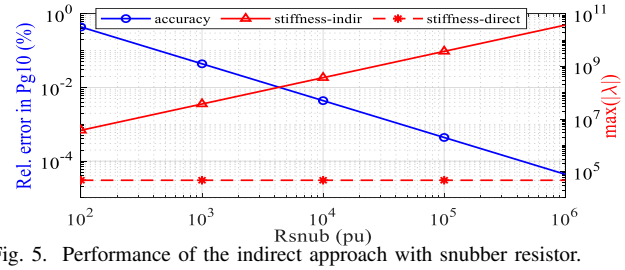

Fig. 5. Performance of the indirect approach with snubber resistor.

coil flux and T_c is the dummy coil open-circuit time constant in the range of a typical damper winding time constant [10]. Table II summarizes the combined models of the SM and transformer with different modeling approaches and SM types.

C. Comparison

Overall, tenth-order model represents the combination of SM and transformer with the indirect snubber as shown in Table II. However, the proposed direct approach requires eighth and ninth-order models for round rotor and salient pole SM respectively (Table II), i.e., it reduces the model order.

IV. CASE STUDIES AND SIMULATION RESULTS

This section validates the proposed direct interfacing approach for the SM and interconnecting transformer models with New England 39-bus test system, shown in Fig. 4. A generator combination of SMs, grid-forming (GFM), and grid-following (GFL) inverters represents the inverter-integrated power system. The system and generator dynamic data is taken from [11]; the inverter topology and control parameters are adapted from [12]. The system is modeled in the *dq* domain with a sixth-order transmission line model. A detailed dynamic modeling is given in [2], [12].

The simulation accuracy is measured in terms of steady-state relative error in power injection of G10 (see Fig. 4) to account for snubber resistance losses and the largest magnitude

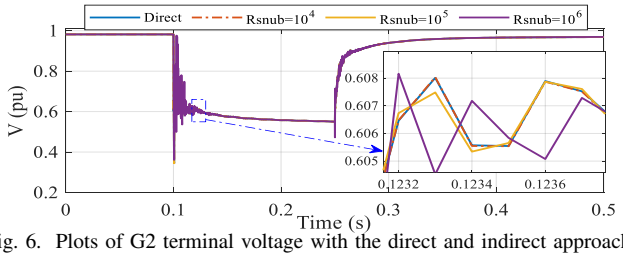

Fig. 6. Plots of G2 terminal voltage with the direct and indirect approaches.

TABLE III
COMPUTATIONAL PERFORMANCE WITH FIXED-STEP SOLVER

Time Step (μs)	Execution Time (s)		Computational gain (%)
	Snubber Approach	Direct Approach	
50	305.03	272.63	11.88
100	154.54	139.75	10.58
200	77.64	70.55	10.05
500	32.03	28.65	11.80

of the eigenvalues measures the model stiffness. An increase in the snubber resistance decreases the snubber losses and improves the steady-state simulation accuracy, but eigenvalues move far away from the origin and increase system stiffness, as shown in Fig. 5. We run simulations on the New England 39-bus system to evaluate this impact on computational performance. The explicit solvers are generally not used in power system simulations due to numerical instability occurring on account of higher model stiffness. So, the following results refer to implicit solvers with fixed or variable time steps.

1) Using Fixed-Step Implicit Solver: This scenario considers a balanced three-phase fault disturbance, shown in Fig. 4, followed by the line trip. A fixed-step second-order implicit MATLAB solver ode14x compares the computational performance of the two approaches for a run time of 0.5 s.

Fig. 6 shows plots of the terminal voltage of the generator, G2, for two approaches with a time step of 100 μs. Although the steady-state simulation accuracy increases with R_{snub} (see Fig. 5), G2 voltage plots show increasing distortions for R_{snub} value of 10^5 p.u. and higher (see Fig. 6) due to increased model stiffness. The graphs overlap with R_{snub} value of 10^4 p.u. and lower, but at the cost of lower steady-state simulation accuracies (see Fig. 5). The distortions in the transient response in Fig. 6 confirms the difficulty in numerical simulations of stiff models, even with implicit solvers.

Table III compares the computational complexity in terms of the simulation execution time with R_{snub} value set to 10^6 p.u. Due to the higher computational complexity, the snubber approach execution time is about 10% higher, as given in Table III. The computational efficiency for the salient pole SMs also comes out in the range of the round rotor SMs, indicating their similar computational complexity, especially in a larger test system. The direct approach is always more efficient, but the computational gain may vary with test systems.

2) Using Variable-Step Implicit Solver: A variable-step implicit solver ode23tb simulates a load change disturbance of 500 MW at bus 4 for 5 s. The tolerance are set to 10^{-6}, and

TABLE IV
COMPUTATIONAL PERFORMANCE WITH VARIABLE-STEP SOLVER

Approach	Snubber					Proposed
R_{snub}	10^2	10^3	10^4	10^5	10^6	-
No. of steps	46193	49470	50048	50327	55688	52881
T_{exe} (s)	48.24	52.2	56.01	65.15	161.9	46.87
T_{exe}/step (ms)	1.044	1.055	1.119	1.295	2.907	0.886
Comp. gain (%)	2.84	10.21	16.32	28.06	71.05	-

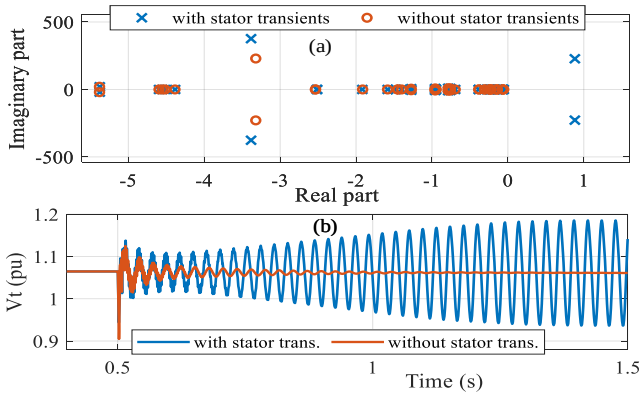

Fig. 7. (a) Low frequency poorly damped modes, (b) GFL2 terminal voltage plots with and without including stator transients with 5% GFL droop gains.

the maximum and minimum time steps are 10^{-2} and 10^{-15}.

Table IV compares the total number of simulation steps and execution time taken by the two approaches. The number of steps, execution time, T_{exe}, and execution time per step increases with R_{snub} value in the case of the snubber strategy. Even though the proposed direct approach takes a higher number of steps as compared to the snubber for R_{snub} values below 10^5 p.u., the execution time for the proposed approach is always lower resulting in a computational gain widely varying between 3% to 71% (see Table IV). The proposed approach is computationally efficient due to the lower computational complexity on the account of reduced model order and stiffness. The model order reduction does not translate into an equal computational gain as it depends upon the model order and stiffness, solver used, and sparsity of the Jacobean matrix.

3) Importance of Including Stator Transients: Fig. 7(a) and (b) show the eigenvalue and GFL2 terminal voltage plots for two cases, i.e., including and neglecting stator transients, with the grid support GFL droop gains decreased from 10% to 5%. It is clear from eigenvalue and voltage plots (see Fig. 7) that neglecting stator transients cannot capture an unstable mode having a frequency of 36.22 Hz. Hence, it is necessary to include SM stator transients to capture complex interactions in stability studies of inverter-integrated power systems.

V. Conclusions

This letter reformulates the detailed multi-time scale SM model as a voltage source behind the sub-transient reactance including stator transients in the *dq* domain, so that it is compatible with the interconnecting transformer model. The presented case studies confirm the superior performance of the proposed direct interfacing approach for SM model in terms of computational efficiency, accuracy, and distortion-less response due to reduced model stiffness. The proposed method has potential use in reliable stability studies of power systems involving complex dynamic interactions with an ever-increasing number of inverters.

References

[1] "Stability definitions and characterization of dynamic behavior in systems with high penetration of power electronic interfaced technologies," IEEE Power & Energy Society, Tech. Rep. PES-TR77, 2020.

[2] U. Markovic, O. Stanojev, P. Aristidou, E. Vrettos, D. Callaway, and G. Hug, "Understanding small-signal stability of low-inertia systems," *IEEE Trans. Power Syst.*, vol. 36, no. 5, pp. 3997–4017, 2021.

[3] P. W. Sauer and M. A. Pai, *Power System Dynamics and Stability*. Prentice Hall, 1998.

[4] L. Wang and et al., "Methods of interfacing rotating machine models in transient simulation programs," *IEEE Trans. Power Del.*, vol. 25, no. 2, pp. 891–903, 2010.

[5] Y. Xia and et al., "An efficient phase domain synchronous machine model with constant equivalent admittance matrix," *IEEE Trans. Power Del.*, vol. 34, no. 3, pp. 929–940, 2019.

[6] L. Wang and J. Jatskevich, "A voltage-behind-reactance synchronous machine model for the emtp-type solution," *IEEE Trans. Power Syst.*, vol. 21, no. 4, pp. 1539–1549, 2006.

[7] M. Chapariha, F. Therrien, J. Jatskevich, and H. W. Dommel, "Explicit formulations for constant-parameter voltage-behind-reactance interfacing of synchronous machine models," *IEEE Trans. Energy Conv.*, vol. 28, no. 4, pp. 1053–1063, 2013.

[8] A. M. Cramer, B. P. Loop, and D. C. Aliprantis, "Synchronous machine model with voltage-behind-reactance formulation of stator and field windings," *IEEE Trans. Energy Conv.*, vol. 27, no. 2, pp. 391–402, 2012.

[9] M. Chapariha, F. Therrien, J. Jatskevich, and H. W. Dommel, "Constant-parameter circuit-based models of synchronous machines," *IEEE Trans. Energy Conv.*, vol. 30, no. 2, pp. 441–452, 2015.

[10] K. R. Padiyar, *Power System Dynamics: Stability and Control*. John Wiley and Sons, Singapore, 1996.

[11] M. A. Pai, *Energy function analysis for power system stability*. Springer Science & Business Media, 1989.

[12] B. Pawar, E. I. Batzelis, S. Chakrabarti, and B. C. Pal, "Modeling and simulation of transients in low inertia power systems," *TechRxiv, Preprint*, 2022. [Online]. Available: https://doi.org/10.36227/techrxiv.19771027.v1